

1 Identification of paleo Arctic winter sea ice limits and the marginal ice zone:
2 optimised biomarker-based reconstructions of late Quaternary Arctic sea ice.

3

4 Simon T Belt^{a,*}, Patricia Cabedo-Sanz^a, Lukas Smik^a, Alba Navarro-

5 Rodriguez^a, Sarah M P Berben^{b,1}, Jochen Knies^{c,d} and Katrine Husum^e

6

7 (a) Biogeochemistry Research Centre, School of Geography, Earth and
8 Environmental Sciences, Plymouth University, Plymouth, PL4 8AA, UK.

9

10 (b) Department of Geology, UiT – The Arctic University of Norway, N-9037
11 Tromsø, Norway

12

13 (c) Geological Survey of Norway, N-7491 Trondheim, Norway.

14

15 (d) CAGE - Centre for Arctic Gas Hydrate, Environment and Climate;
16 Department of Geology, University of Tromsø, N-9037 Tromsø, Norway.

17

18 (e) Norwegian Polar Institute, Fram Centre, NO-9296 Tromsø, Norway.

19

20

21 * Author for correspondence

22 e-mail: sbelt@plymouth.ac.uk

23

24

25 Keywords: Sea ice; Arctic; Proxy; IP₂₅; Biomarker; Paleoclimate

26

27

¹ Current Address: Department of Earth Science and the Bjerknes Centre for Climate Research, University of Bergen, N-5007 Bergen, Norway.

28 **Abstract**

29 Analysis of >100 surface sediments from across the Barents Sea has shown
30 that the relative abundances of the mono-unsaturated sea ice diatom-derived
31 biomarker IP₂₅ and a tri-unsaturated highly branched isoprenoid (HBI) lipid
32 (HBI III) are characteristic of the overlying surface oceanographic conditions,
33 most notably, the location of the seasonal sea ice edge. Thus, while IP₂₅ is
34 generally limited to locations experiencing seasonal sea ice, with higher
35 abundances found for locations with longer periods of ice cover, HBI III is
36 found in sediments from all sampling locations, but is significantly enhanced in
37 sediments within the vicinity of the retreating sea ice edge or marginal ice
38 zone (MIZ). The response of HBI III to this well-defined sea ice scenario also
39 appears to be more selective than that of the more generic phytoplankton
40 biomarker, brassicasterol. The potential for the combined analysis of IP₂₅ and
41 HBI III to provide more detailed assessments of past sea ice conditions than
42 IP₂₅ alone has been investigated by quantifying both biomarkers in three
43 marine downcore records from locations with contrasting modern sea ice
44 settings. For sediment cores from the western Barents Sea (intermittent
45 seasonal sea ice) and the northern Norwegian Sea (ice-free), high IP₂₅ and
46 low HBI III during the Younger Dryas (ca. 12.9–11.9 cal. kyr BP) is consistent
47 with extensive sea cover, with relatively short periods of ice-free conditions
48 resulting from late summer retreat. Towards the end of the YD (ca. 11.9–11.5
49 cal. kyr BP), a general amelioration of conditions resulted in a near winter
50 maximum ice edge scenario for both locations, although this was somewhat
51 variable, and the eventual transition to predominantly ice-free conditions was
52 later for the western Barents Sea site (ca. 9.9 cal. kyr BP) compared to NW

53 Norway (ca. 11.5 cal. kyr BP). For both locations, coeval elevated HBI III (but
54 absent IP₂₅) potentially provides further evidence for increased Atlantic Water
55 inflow during the early Holocene, but this interpretation requires further
56 investigation. In contrast, IP₂₅ and HBI III data obtained from a core from the
57 northern Barents Sea demonstrate that seasonal sea ice prevailed throughout
58 the Holocene, but with a gradual shift from winter ice edge conditions during
59 the early Holocene to more sustained ice cover in the Neoglacial; a directional
60 shift that has undergone a reverse in the last ca. 150 yr according to
61 observational records. Our combined surface and downcore datasets suggest
62 that combined analysis of IP₂₅ and HBI III can provide information on temporal
63 variations in the position of the maximum (winter) Arctic sea ice extent,
64 together with insights into sea ice seasonality by characterisation of the
65 MIZ. Combining IP₂₅ with HBI III in the form of the previously proposed PIP₂₅
66 index yields similar outcomes to those obtained using brassicasterol as the
67 phytoplankton marker. Importantly, however, some problems associated with
68 use of a variable balance factor employed in the PIP₂₅ calculation, are
69 potentially alleviated using HBI III.

70 **1. Introduction**

71 Sea ice plays a major role in controlling the energy budget at the Earth's
72 surface by reflecting a significant part (>90%) of incoming radiation due to the
73 so-called albedo effect. Sea ice also acts as a physical barrier to heat and gas
74 exchange between the oceans and the atmosphere, and contributes to ocean
75 circulation through brine release during formation and freshwater discharge
76 during melting (e.g. Dickson et al., 2007 and references therein). It also
77 experiences large seasonal variations and inter-annual variation can also be
78 significant. Variations in sea ice also influence climate change scenarios
79 beyond the polar regions through tele-connections (e.g. Wang et al., 2005).
80 However, despite recognition of the key roles that sea ice plays in global
81 climate, with recent reductions in extent and thickness attracting considerable
82 attention (e.g. Stroeve et al., 2012), long term records of sea ice and
83 variations in its distribution have, until recently, remained relatively scarce,
84 principally due to a combination of the logistical constraints of working in the
85 polar regions and a lack of suitable (proxy) methodologies. Observational
86 records of past sea ice are spatially incomplete and, in any case, rarely
87 extend beyond a few hundred years (Divine and Dick, 2006), while
88 reconstructions based on geological archives are particularly challenging since
89 sea ice leaves no direct legacy signature in marine or terrestrial records;
90 however, a number of proxy methods have been developed to specifically
91 address this. Some of these approaches are based on the responses of
92 pelagic or benthic organisms whose distributions and composition (e.g. stable
93 isotopes) are influenced by sea ice cover (for an overview, see de Vernal et
94 al., 2013 and references therein), while others rely on the identification of

95 material entrained within the sea ice itself (i.e. ice-rafted debris (IRD)) which is
96 deposited in sediments following release from melting ice (Andrews, 2009).
97
98 In recent years, the analysis of the biomarker IP₂₅ (structure I; Fig. 1; Belt et
99 al., 2007), a C₂₅highly branched isoprenoid (HBI) lipid made uniquely by
100 certain Arctic sea ice-dwelling diatoms (Brown et al., 2014), has been
101 suggested to provide a more direct measure of past sea ice when detected in
102 underlying sediments (see Belt and Müller, 2013 for a recent review).
103 Importantly, IP₂₅ has been identified in sediments from a large number of
104 surface sediments from seasonally ice-covered Arctic locations and downcore
105 records spanning timescales from recent decades (Müller et al., 2011;
106 Stoyanova et al., 2013; Xiao et al., 2013; Navarro-Rodriguez et al., 2013), the
107 Holocene (Vareet et al., 2009; Müller et al., 2012) and even longer (Stein and
108 Fahl, 2013; Knies et al., 2014; Müller and Stein, 2014). A remaining question,
109 however, concerns the extent to which the analysis of IP₂₅ can provide more
110 detailed or quantitative estimates of paleo sea ice. Initially, Massé et al.
111 (2008) demonstrated that IP₂₅ abundances in a marine core from the North
112 Icelandic Shelf exhibited a strong relationship to known sea ice conditions in
113 observational records and, in general, changes in sedimentary concentrations
114 of IP₂₅ are consistent with corresponding variations in sea ice extent (Belt and
115 Müller, 2013). Absolute abundances of IP₂₅, however, vary considerably
116 between different Arctic regions with otherwise similar sea ice extent and no
117 strict relationship with sea ice concentration exists. Despite this limitation, the
118 selectivity of sedimentary IP₂₅ to seasonally ice-covered locations largely
119 remains, making its presence a useful qualitative sea ice proxy, at least.

120 Exceptionally, IP₂₅ has been identified in a small number of sediments from
121 either ice-free locations or those from near permanent ice cover, although
122 these are likely explained by sediment advection and (at least) partial ice melt,
123 respectively (Navarro-Rodriguez et al., 2013; Xiao et al., 2015).

124

125 In order to distinguish between the two extreme scenarios of ice-free
126 conditions and permanent ice cover, more generally, Müller et al. (2009)
127 suggested the parallel measurement of pelagic phytoplankton biomarkers that
128 might be considered indicators of ice-free sea surface conditions. As such, the
129 absence or low abundance of phytoplankton sterol lipids such as
130 brassicasterol may serve to indicate permanent sea ice coverage, while
131 elevated brassicasterol content would suggest predominantly ice-free
132 conditions. The success of this approach in reconstructing sea ice conditions for
133 the Fram Strait over the last 30 kyr (Müller et al., 2009) led to the subsequent
134 development of the so-called PIP₂₅ index, whereby concentrations of IP₂₅ and
135 a phytoplankton biomarker (typically brassicasterol) are combined to provide
136 semi-quantitative estimates of sea ice concentration (Müller et
137 al., 2011). However, although relationships between PIP₂₅ data and sea ice
138 concentrations are, in general, better than those using IP₂₅ alone (e.g. Xiao et
139 al., 2015), this is not always the case (Navarro-Rodriguez et al., 2013) and the
140 underlying reasons for such improved correlations are not fully resolved, not
141 least due to the uncertainties in the true inter-relationship between IP₂₅ and
142 phytoplankton lipids under different sea ice settings, or the strict pelagic origin
143 of brassicasterol in all cases (e.g. Fahl and Stein, 2012; Belt et al., 2013; Xiao
144 et al., 2015).

145

146 An alternative approach may be better focussed on improving our
147 understanding of different sea ice *conditions* (e.g. seasonal ice, drift ice) rather
148 than sea ice *concentrations*, especially if biological processes, and signatures
149 of these, are particularly characteristic of the former. Indeed, establishing
150 parameters such as the winter/summer ice margins or sea ice seasonality are
151 especially important since they are used as boundary parameters in climate
152 forecasting and hindcasting models. In this respect, PIP₂₅ data have also
153 been interpreted in terms of categorisation of sea ice conditions (Müller et al.,
154 2011) although further caveats also exist. Amongst its identified limitations
155 (see Belt and Müller (2013) for a comprehensive review), the variable sources
156 of brassicasterol and the potential lack of sensitivity of its production to
157 individual environmental settings make reconstruction of different sea ice
158 conditions rather challenging, for certain regions at least. For example,
159 brassicasterol may have influences from pelagic, sea ice, freshwater and
160 terrestrial input (Huang and Meinschein, 1976; Volkman, 1986; Fahl and Stein,
161 2012; Belt et al., 2013; Xiao et al., 2015), while abundances in Barents Sea
162 surface sediments were not substantially different between seasonally ice-
163 covered and year-round ice-free locations (Navarro-Rodriguez et al., 2013). A
164 further issue, when using phytoplankton sterols as indicators of the open-
165 water setting, concerns the so-called balance factor (*c*) used in the PIP₂₅
166 calculation, and employed to accommodate the (generally) substantially
167 higher sedimentary concentrations of sterols compared to IP₂₅. In particular,
168 since the magnitude of *c* is dependent on both the number and nature of the
169 samples from which it is derived, outcomes from surface calibrations and

170 downcore records may be modified dramatically, for example, simply on the
171 basis of which sedimentary sections are being analysed. Recently, Xiao et al
172 (2015) suggested that a global c factor might be more useful in this respect;
173 however, the occurrence of significant regional differences emphasizes that
174 selection of the most appropriate value remains problematic.

175

176 A related strategy conceivably involves the analysis of a different lipid
177 biomarker that, like IP_{25} , has a well-defined or constrained source, whose
178 production is more closely aligned with certain pelagic (or sea ice) conditions,
179 and has sedimentary concentrations closer to those of IP_{25} , thus potentially
180 removing the need to employ a balance factor when calculating PIP_{25} indices.

181 In the current study, we apply this approach using a further C_{25} HBI
182 lipid, which, like IP_{25} , is believed to be biosynthesised by a relatively small
183 number of marine diatom genera yet, in contrast to IP_{25} , does not appear to
184 be biosynthesised by sea ice diatoms or other sources. This tri-unsaturated
185 HBI (HBI III; Fig. 1) is found commonly in marine sediments from temperate
186 settings worldwide (Belt et al., 2000) and also in Antarctic phytoplankton and
187 sediments (Massé et al., 2011). Indeed, HBI III has been further hypothesised
188 to represent a potential proxy for the pelagic environment adjacent to
189 retreating sea ice or the marginal ice zone (MIZ) in the Antarctic (Collins et al.,
190 2013). Such a hypothesis was based on the similarities in temporal profiles
191 within Scotia Sea sediments, of HBI III and a di-unsaturated HBI (HBI II; Fig.
192 1), considered to be a sea ice proxy in the Antarctic (Massé et al., 2011;
193 Collins et al., 2013). However, the analyses of surface sediments or

194 phytoplankton from such locations to support this hypothesis further have not,
195 as yet, been presented.

196

197 Here, we analysed biomarker lipids (IP₂₅, HBI III and brassicasterol) in surface
198 and downcore sediment material from locations across the Barents Sea, in
199 part, because the region has a reasonably well-defined annual sea ice
200 advance/retreat cycle, and also since complementary observational and proxy
201 data were available. In addition, Vare et al. (2010) demonstrated that
202 abundances of IP₂₅ in dated short cores from the region aligned well with
203 observational sea ice records covering the last few hundred years.

204 Comparison of our findings from surface sediments with those of downcore
205 records suggests that combined analysis of IP₂₅ and HBI III can be used
206 to characterise the maximum (winter) sea ice extent and MIZ, in particular, thus
207 providing more detailed information regarding paleo sea ice conditions than
208 through analysis of IP₂₅ (or PIP₂₅) alone.

209

210 **2. Regional setting**

211 The Barents Sea is a relatively shallow (mean depth 230 m) epicontinental
212 shelf between the north Norwegian coast and the Svalbard archipelago that
213 plays a crucial role in the Arctic climate system, largely, since it contributes to
214 significant heat exchange between the ocean and the atmosphere (Serreze et
215 al., 2007). Detailed descriptions of the main surface currents in the Barents
216 Sea (and the adjacent northern Norwegian Sea) can be found elsewhere
217 (Loeng, 1991) and a summary is shown in Fig. 2a. In brief, the North Atlantic
218 Current (NAC) delivers relatively warm salty Atlantic water (>2°C; >35‰;

219 Hopkins, 1991) into the northern North Atlantic (Swift, 1986) before dividing
220 into the West Spitsbergen Current (WSC) and the North Cape Current
221 (NCaC) which provide inflow to the Arctic Ocean and the Barents Sea,
222 respectively, with a further branch of the NCaC flowing parallel with the coastal
223 current system (Loeng, 1991). In contrast, colder and less saline Polar water
224 ($0-2^{\circ}\text{C}$; $33-34.4\text{‰}$; Hopkins, 1991) is brought into the Atlantic Ocean from the
225 Arctic Ocean by the East Greenland Current (EGC) and into the Barents Sea
226 by the East Spitsbergen Current (ESC) and Bear Island Current (BIC). Polar
227 and Atlantic water meet in the Barents Sea to form Arctic water (ca. 0.5°C ; ca.
228 34.8‰ ; Hopkins, 1991), which is characterized by reduced temperature and
229 salinity, as well as the occurrence of seasonal sea ice (Hopkins, 1991). Warm
230 and fresh coastal water ($2-13^{\circ}\text{C}$, $32-35\text{‰}$; Hopkins, 1991) is found on the
231 shelves and off the coast of Norway and is transported northwards by the
232 Norwegian Coastal Current (NCC) into the South-West Barents Sea and
233 along the Norwegian and Russian coastline (Aure and Strand, 2001).

234

235 Of particular significance to this region, the boundaries between Polar/Arctic
236 and Arctic/Atlantic waters correspond to the Polar Front and Arctic Front,
237 respectively, both of which represent a sharp climatic gradient in terms of
238 temperature, salinity and sea ice coverage (Hopkins, 1991). The overall
239 extent of sea ice distribution in the northern North Atlantic and the Barents
240 Sea, therefore, is closely related to the positions of the Polar and Arctic
241 Fronts, which represent the average summer and winter sea ice margins,
242 respectively (Vinje, 1977). Consequently, sea ice is formed during autumn
243 and winter in the north-eastern Barents Sea (Loeng, 1991), while the southern

244 Barents Sea is characterized by large seasonal and inter-annual sea ice
245 distribution changes, largely due to the strong (and variable) influence of
246 inflowing Atlantic Water (AW) (Kvingedal, 2005). Such changes in sea ice can
247 be readily seen by the locations of the maximum, minimum and median April
248 sea ice extent for the period 1980-2015 derived from satellite data (NSIDC;
249 Fig. 3). A significant contribution to the annual primary production in the
250 Barents Sea results from a peak algal bloom during the spring as ice retreats
251 along the ice edge or MIZ (Sakshaug et al., 2009).

252

253 **3. Material and methods**

254 *3.1. Surface sediment material*

255 Surface sediment samples were collected and analysed from a broad range of
256 locations within the Barents Sea (Fig. 2b) using box cores, multicores and
257 gravity cores. The majority of the surface sediment samples (0–1 cm) have
258 been described elsewhere (Navarro-Rodriguez et al., 2013) and these have
259 been supplemented for the current study with additional samples from the
260 MAREANO program (Knies and Martinez, 2009) and further material collected
261 on-board the *James Clark Ross* (UK) and the *Polarstern* (Germany) research
262 vessels during oceanographic cruises JR142 and ARK-VIII/2 in 2006 and
263 1991, respectively. A summary of all core locations and biomarker data can
264 be found in Supplementary Table 1.

265

266 *3.2. Downcore sediment material*

267 Descriptions of the marine sediment cores analysed for the temporal part of
268 this study (including core chronologies) can also be found in detail

269 elsewhere. Briefly, core JM99-1200 was collected from the Andfjorden,
270 northern Norway (69.16° N, 16.25° E) and is described in Ebbesen and Hald
271 (2004), Knies (2005) and Cabedo-Sanz et al. (2013). Core NP05-11-70GC
272 was retrieved from the Olga Basin, northern Barents Sea (78.40° N, 32.42° E)
273 and has been described previously by Berben (2014). Finally, core JM09-
274 KA11-GC was collected from the Kveithola Trough, western Barents Sea
275 (74.87° N; 16.48° E), and details can be found in R  ther et al. (2012) and
276 Berben et al., (2014). The age model for JM09-KA11-GC used in Berben et al.
277 (2014) has been supplemented using a further ¹⁴C date (ca. 13.12 cal. kyr BP;
278 R  ther et al., 2012) in order for us to be able to extend the biomarker record
279 to cover the Younger Dryas (YD). Hereafter, cores JM99-1200, NP05-11-
280 70GC and JM09-KA11-GC are referred to as 1200, 70 and 11, respectively.

281

282 3.3. Biomarker analyses

283 Details of the extraction and analysis of HBI and sterol lipids described herein
284 can be found elsewhere (Belt et al., 2012, 2013). Briefly, ca. 1–5 g of freeze
285 dried sediment material was extracted (dichloromethane/methanol; 3 x 3 mL;
286 2:1 v/v) by ultrasonication following addition of internal standards (9-
287 octylheptadec-8-ene (10 µL; 1 µg mL⁻¹) and 5α-androstan-3β-ol (10 µL; 1 µg
288 mL⁻¹) for the quantification of HBI lipids and brassicasterol, respectively.

289 Where necessary, elemental sulfur was removed from the resulting total
290 organic extracts (TOEs) (Cabedo-Sanz and Belt, 2015) and these partially
291 purified TOEs were then separated into fractions containing HBIs and sterols
292 as described previously (e.g. Belt et al., 2012). Fractions containing
293 brassicasterol were derivatized using N,O-Bis(trimethylsilyl)trifluoroacetamide

294 (BSTFA, 50 μ L, 70 $^{\circ}$ C; 1h). All fractions were analysed using gas
295 chromatography–mass spectrometry (GC–MS) with operating conditions as
296 described by Belt et al. (2012). Identification of individual lipids was based on
297 their characteristic GC retention times and mass spectra compared with those
298 of reference compounds, while quantification was achieved by comparison of
299 peak area integrations of selected ions (m/z 350 (IP₂₅); 346 (HBI III); 470
300 (brassicasterol)) with those of the internal standard in selected ion monitoring
301 (SIM) mode (Belt et al., 2012). These ratios were normalized to instrumental
302 response factors obtained for individual lipids and sediment mass (Belt et al.,
303 2012). Our data comprise some previously reported concentrations of IP₂₅ and
304 brassicasterol in surface sediments from the Barents Sea (Navarro-Rodriguez
305 et al., 2013) and these have been supplemented by some new data obtained
306 as part of the current study. All of the HBI III concentration data are new to
307 this study. We have also confined our dataset to those locations for which we
308 have IP₂₅ and HBI III concentrations data, at least, and all three biomarkers
309 for the majority of locations. Exceptionally, brassicasterol was not measured
310 in a small number of surface sediments from NW Norway. PIP₂₅ values were
311 calculated using the formula $PIP_{25} = IP_{25}/(IP_{25}+cP)$, with individual terms as
312 described by Müller et al. (2011). Two-tailed t-tests were performed and
313 interpreted (95% confidence limits) for statistical analyses.

314

315 3.4. Sea ice data

316 In order to place our biomarker data into a spatial and recent temporal sea ice
317 context, we obtained estimates of sea ice extent using polyline shapefiles
318 derived from satellite data collected for the period 1981-2010 (NSIDC). From

319 these, we identified the individual years of (overall) maximum and minimum
320 extent for April (winter maximum), and the median position of the maximum
321 (April) and minimum (September) ice edge. This interval is suitable for
322 contextualising surface (typically 0–1 cm) sediment data since accumulation
323 rates in the region are generally of the order of 1 cm yr⁻¹ (Maitiet al., 2010;
324 Vare et al., 2010).

325

326 **4. Results and discussion**

327

328 *4.1. Biomarkers in surface sediments – characterisation of the winter ice edge* 329 *and the MIZ*

330

331 In total, 102 surface sediment samples were analysed for IP₂₅ and HBI III. Of
332 these, 75 were also analysed for brassicasterol. Consistent with previous
333 findings, the sea ice biomarker IP₂₅ was identified in 44 out of 45 (98%)
334 extracts obtained from seasonally ice-covered locations (Fig. 3a).

335 Exceptionally, IP₂₅ was also identified in a few (7 out of 57; 13%) sediments
336 from locations south of the maximum winter sea ice extent and this has been
337 attributed, previously, to some likely allochthonous input or sediment
338 advection from locations further up the slope (Navarro-Rodriguez et al., 2013)
339 rather than local (autochthonous) production. In addition, the mean IP₂₅
340 concentration for locations further north of the median April sea ice edge, with
341 ice also persisting past June (5.5±3.3 ng g⁻¹; n=22), was significantly higher
342 (p=0.01) than for locations proximal to the winter sea ice edge (3.1±2.5 ng g⁻¹;
343 n=23). We interpret these findings as indicating enhanced IP₂₅ production

344 (and subsequent deposition) for areas experiencing longer seasonal sea ice
345 cover, with melt only occurring during late summer, while lower sedimentary
346 IP₂₅ abundances are found for locations that do not always experience sea ice
347 cover on an annual basis and where spring-summer ice retreat occurs earlier
348 (e.g. May–June). Consistent with this difference, IP₂₅ is normally absent (or
349 below the limit of detection) for the majority of locations beyond the maximum
350 winter sea ice margin.

351

352 Some quite different trends are apparent from the HBI III data, however. For
353 example, in contrast to IP₂₅, HBI III was present in virtually all (101 out of 102;
354 99%) of the sediment extracts, consistent with a pelagic phytoplankton origin
355 for this biomarker rather than sea ice diatoms. Indeed, as far as we are
356 aware, HBI III has, to date, not been identified in Arctic sea ice. Concentrations
357 of HBI III were relatively low for regions that experience annual and extensive
358 sea ice cover (mean $0.40 \pm 0.38 \text{ ng g}^{-1}$; Fig 3b), which contrasts the enhanced
359 IP₂₅ abundances for the same locations (Fig. 3a), likely as a consequence of
360 shorter (and cooler) summer seasons with lower phytoplankton productivity
361 (Sakshaug et al., 2009). A somewhat higher mean HBI III concentration
362 ($1.7 \pm 1.6 \text{ ng g}^{-1}$; $n=57$) was found for ice-free locations in the southern (and
363 warmer) region of sampling consistent with increased productivity in this region
364 (Sakshaug et al., 2009). When compared against both of these two regions,
365 however, a significantly higher ($p < 0.001$) mean HBI III concentration (13.0 ± 8.3
366 ng g^{-1} ; $n=23$) was observed for locations bordered by the minimum (2006) and
367 maximum (1981) April ice margins (Fig. 3b). The enhancement of HBI III in
368 this region, especially relative to locations further north, represents a clear

369 reversal in trend compared to IP_{25} , and suggests increased production during
370 late spring/early summer, which is reduced for locations with longer lasting
371 sea ice cover. However, it is also evident that the mean HBI III concentration
372 for this region of retreating ice edge is substantially (ca. 7–8 times) higher
373 than for the annually ice-free locations, and is thus indicative of the well-
374 known enhanced phytoplankton production within the MIZ as sea ice retreats
375 during late spring (April-May) and into early summer (June) (Sakshauget al.,
376 2009).

377

378 In order to assess whether the trends observed for HBI III could be identified
379 through other pelagic productivity indicators, we considered the distribution
380 pattern for the phytoplankton marker brassicasterol (Fig. 3c). In accord with
381 the trends identified for HBI III, the mean brassicasterol concentration was
382 lowest for the region with most persistent sea ice cover ($375 \pm 177 \text{ ng g}^{-1}$;
383 $n=22$), slightly higher for ice-free settings ($695 \pm 1200 \text{ ng g}^{-1}$; $n=33$), and
384 highest for locations within the MIZ ($1470 \pm 1200 \text{ ng g}^{-1}$; $n=20$). However, the
385 relative changes between the three regions were clearly greater for HBI III
386 than for brassicasterol. Most noticeably, the mean enhancement of HBI III
387 between the MIZ and the region with more extended seasonal ice cover
388 ($\times 32.5$) was more than eight times that of brassicasterol ($\times 3.9$),
389 probably because the latter is a common component in marine phytoplankton
390 and its distribution pattern reflects productivity spanning all growth seasons,
391 while the former is likely biosynthesised by a much smaller number of
392 sources, but whose growth is especially favoured by, or at least more tolerant
393 to, the nutrient-rich and stratified upper water column found at the ice-edge.

394 The differences in distribution of brassicasterol between regions may be
395 further complicated or blurred by production of this sterol in certain sea ice
396 diatoms (e.g. Belt et al., 2013) and other sources (Volkman, 1986), especially
397 for locations that may receive contributions from terrestrial sources (Huang
398 and Meinschein, 1976; Volkman, 1986; Fahl and Stein, 2012; Xiao et al.,
399 2015). In contrast, although the exact sources of HBI III in the study region
400 have not been firmly identified, the only known producers of this biomarker are
401 marine diatoms within the genera *Pleurosigma* (Belt et al., 2000) and
402 *Rhizosolenia* (Rowland et al., 2001). Further, when measured in Arctic marine
403 sediments, HBI III has a stable isotopic composition ($\delta^{13}\text{C}$ ca. -35 to -40 ‰;
404 Belt et al., 2008) consistent with a polar phytoplanktic origin (Massé et al.,
405 2011) where cold and CO_2 -enriched waters can result in highly depleted ^{13}C
406 composition (Tolosa et al., 2013).

407

408 In summary, our surface sediment data reinforce the view that the biomarker
409 IP_{25} has a highly selective sea ice diatom origin, with sedimentary
410 abundances enhanced for regions experiencing more frequent and longer-
411 lasting spring sea ice cover. In contrast, HBI III is common to all seasonally
412 ice-free regions, but is especially enhanced in sediments for locations that
413 reflect the retreating ice edge or MIZ during late spring-summer. Such
414 observations are likely driven by the individual diatom genera responsible for
415 the biosynthesis of IP_{25} and HBI III, while the distinctive differences in their
416 stable isotopic composition confirms the contrasting environments in which
417 they are produced.

418

419 *4.2 Temporal biomarker profiles and identification of sea ice conditions*

420 In order to establish whether the data and outcomes from the surface
421 sediment analyses could be used to provide more detailed descriptions of sea
422 ice conditions over longer timescales, we analysed IP₂₅, HBI III and
423 brassicasterol in three well-dated marine sequences from locations with
424 contrasting modern sea ice cover (*viz.* long-lasting seasonal ice, inter-annual
425 ice edge, ice-free) and compared outcomes with our surface sediment data
426 and previous findings.

427

428 *4.2.1. Olga Basin (northern Barents Sea)*

429 Core 70 was retrieved from the Olga Basin in the northern Barents Sea, a
430 location that, in modern times, experiences annual sea ice cover that forms
431 during autumn/winter. Ice retreat occurs during the summer such that the site
432 is normally only ice-free during August and September (Fig. 2b). Our
433 biomarker record for core 70 covers the last ca. 9.5 cal. kyr BP. IP₂₅
434 concentration (Fig. 4a) is low during the early part of the record and increases
435 steadily towards recent times, with a core-top value similar to that found in
436 nearby surface sediments (Navarro-Rodriguez, 2014). An opposite trend is
437 observed for HBI III (Fig. 4b), however, with highest concentrations occurring
438 in the early Holocene and a decline towards the recent record, where values
439 (ca. 1 ng g⁻¹) are also within the range found for nearby surface sediments
440 (ca. 0.1–1.6 ng g⁻¹; Fig. 3b). A small decline in the brassicasterol
441 concentration is also observed (Fig. 4c), but this is not as pronounced as for
442 HBI III, possibly due to a lower sensitivity to the overlying sea ice conditions
443 as demonstrated through our surface sediment data.

444

445 Previously, Berben (2014) suggested that these IP₂₅ and brassicasterol data
446 indicated seasonal sea ice cover throughout the record, but with shorter
447 spring sea ice cover and longer (and warmer) summers during the early
448 Holocene. These conclusions were supported further by the species
449 distribution, preservation state and isotopic composition of planktic
450 foraminifera. Berben (2014) also hypothesised that the position of the
451 winter/spring ice-edge was in the proximity of the core 70 site during the early
452 Holocene before advancing south and towards the modern sea ice limit after
453 ca. 6.5 cal. kyr BP. Significantly, therefore, we observe elevated HBI III during
454 the early Holocene (ca. 9.5–8.5 cal. kyr BP), during which time, the mean
455 concentration (ca. 11 ng g⁻¹) resembles that found for the modern sea ice edge
456 locations (13.0 ng g⁻¹). At the same time, lower (compared to modern) IP₂₅
457 concentrations are also consistent with a modern winter/spring scenario. As
458 such, the combined IP₂₅ and HBI III data for core 70 in the early Holocene
459 reflect sea ice edge conditions normally associated with locations further south
460 during modern times. Similarly, by consideration of the contrasting responses
461 between IP₂₅ and HBI III in surface sediments, together with the reversal in
462 temporal profiles for IP₂₅ and HBI III, we confirm a gradual lengthening in
463 seasonal ice duration over the core location throughout the Holocene (Berben,
464 2014), with progressively shorter (and cooler) summer seasons.

465

466 4.2.2. Kveithola Trough (western Barents Sea)

467 In contrast to the Olga Basin site, core 11 was obtained from a location in the
468 western Barents Sea close to the modern maximum winter sea ice extent and

469 thus experiences variable sea ice cover (presence/absence) on an annual
470 basis and, in any case, for shorter periods (e.g. November–April). Consistent
471 with such differences, IP₂₅ concentrations in surface sediments from the
472 western Barents Sea are much lower than those for the northern Barents Sea
473 (Fig. 3a). Previously, Berben et al. (2014) reported relatively low abundances
474 of IP₂₅ in core 11 throughout the Holocene, although slightly elevated values
475 were noted for the last ca. 1.0 cal.kyr BP, consistent with late Holocene
476 increases in spring sea ice extent. However, relatively high IP₂₅ and
477 brassicasterol abundances were noted during the interval ca. 10.8–10.3 cal.
478 kyr BP, while even higher IP₂₅(but lower brassicasterol) concentrations were
479 observed in the earliest part of the record (ca. 11.9–10.8 cal. kyr BP). These
480 were interpreted as reflecting, respectively, stable MIZ conditions (favourable
481 for both biomarkers) during the early Holocene, which was preceded by a
482 period of more extensive sea ice cover during the latter stages of the YD. Our
483 data here extend those of Berben et al. (2014), with new IP₂₅ data for the YD
484 (to ca. 13.0 cal. kyr BP), and HBI III concentrations for the entire record, thus
485 providing either clarification or further detail to these previous interpretations
486 (Fig. 5). For example, during the majority of the YD (ca. 13 – 11.9 cal. kyr BP),
487 IP₂₅ concentrations are at their highest values throughout the entire record,
488 after which, a reduction is observed beginning ca. 11.9 cal.kyr BP, before
489 reaching consistently lower levels ca. 11.3 cal. kyr BP (Fig. 5a). The elevated
490 IP₂₅ concentration during the YD is accompanied by extremely low HBI III
491 abundance which, according to our surface datasets, is indicative
492 of consistently long seasonal sea ice cover characteristic of the northern
493 Barents Sea in modern times (Figs. 3a, 3b). In contrast, lower IP₂₅ and

494 intermittently higher HBI III concentrations can be seen for the period ca.
495 11.5–9.9 cal. yr BP, signifying stable ice edge or MIZ conditions. However, the
496 variability in the HBI III abundance, in particular, suggests that such winter ice
497 edge conditions probably did not prevail throughout the entire interval but
498 were more intermittent, with relatively frequent short-term changes compared
499 to the northern Barents Sea (core 70). Indeed, large temperature shifts have
500 been recorded previously for the western Barents Sea during this
501 interval, consistent with a high degree of climatic variability (Hald et al., 2007).
502 Our data suggest, therefore, that the most severe sea ice conditions for this
503 site only existed during the YD, with reasonably similar-to-modern conditions
504 reached by the early Holocene, whereupon they remained reasonably
505 consistent. Thus, for the majority of the Holocene sections after ca. 7.8 cal. yr
506 BP, IP₂₅ was either very low in concentration or absent (Fig. 5a), while the
507 abundance of HBI III (Fig. 5b) was also lower than that observed in the
508 aforementioned intervals and similar to those seen for surface sediments from
509 ice-free locations further south (Figs. 3a, 3b), indicating only infrequent sea
510 ice cover at the core location. Exceptionally, during the early Holocene (ca.
511 9.9–7.8 cal. kyr BP), absent IP₂₅ (or below our limit of detection) is
512 accompanied by relatively high HBI III concentrations, although this is not the
513 case for brassicasterol (see Section 4.2.5 for a discussion of this observation).
514 For this core, reduced brassicasterol during the YD followed by elevated
515 levels ca. 11.5–9.9 cal kyr BP (Fig. 5c) also support the notion of a transition
516 from long seasonal ice cover to ice-edge conditions; however, there are also
517 some out-of-phase changes within the brassicasterol and HBI III profiles

518 during this interval, likely further reflecting the reduced selectivity of the
519 former and input from a range of sources.

520

521 4.2.3. Andfjorden (northern Norwegian Sea)

522 Our third case study (core 1200) represents a location in the northern
523 Norwegian Sea and is thus significantly further south of the modern winter sea
524 ice edge (Fig. 2). Not surprisingly, therefore, IP₂₅ is absent in all surface
525 sediments from nearby locations along the NW Norwegian coast (Fig. 3a).
526 However, in a previous study, Cabedo-Sanz et al. (2013) demonstrated that
527 the site was covered by extensive seasonal sea ice during the YD through
528 identification of elevated IP₂₅ levels between ca. 12.9–11.9 cal.kyr BP, but
529 was ice-free (IP₂₅ absent) throughout the early-mid Holocene (ca. 11.5–6.3
530 cal. kyr BP). During the termination of the YD (ca. 11.9–11.5 cal.kyr BP),
531 significantly lower IP₂₅ abundance compared to the previous millennium
532 was hypothesised to reflect reduced/more variable sea ice conditions or shorter
533 seasonal sea ice cover, but this was not investigated further. Here, we show
534 that, consistent with the conclusions of Cabedo-Sanz et al. (2013) and our
535 observations for core 11 (western Barents Sea), HBI III concentrations (Fig.
536 6b) are extremely low throughout the interval of elevated IP₂₅ abundances
537 during the YD (ca. 12.9–11.9 cal.kyr BP), indicative of extensive sea ice extent
538 associated with harsh winters and only short (ice-free) summers. Such
539 conclusions are also in-line with low SST (Ebbesen and Hald, 2004) and other
540 biogenic proxy data (Knies, 2005) obtained from the same core. Interestingly,
541 during the subsequent period, with lower IP₂₅, HBI III concentrations increase
542 markedly, albeit with some fluctuations in absolute values, including a zero

543 value at ca. 11.75 cal. kyr BP, coeval with absent IP₂₅ and brassicasterol (Fig.
544 6), and interpreted previously as a short interval of extreme climate with
545 permanent ice cover (Cabedo-Sanz et al., 2013). In general, however, we
546 interpret this switch in relative abundances of IP₂₅ and HBI III to indicate a
547 transition from extensive sea ice cover, with only short intervals of ice-free
548 cover during summers, from ca. 12.9–11.9 cal. kyr BP, to one of a (variable)
549 winter ice edge scenario over the core location (and progressive retreat from
550 this) from 11.9–11.5 cal. kyr BP, similar to what we propose for the western
551 Barents Sea (core 11). This represents a modification to the interpretation of
552 PIP₂₅ data derived from core 1200 described previously (Cabedo-Sanz et al.,
553 2013), where MIZ conditions were indicated for the majority of the YD (ca.
554 12.9–11.9 cal. kyr BP). However, PIP₂₅ values (and the interpretations thereof)
555 can be subject to considerable variability, especially as a consequence of
556 changes to the balance factor, whose magnitude can be strongly influenced
557 by the temporal range of the core intervals being considered (see Introduction,
558 section 4.2.4 and Belt and Müller, 2013). In addition, the brassicasterol data
559 for core 1200 do not reveal such clearly contrasting sea ice conditions as IP₂₅
560 and HBI III, with alternating high and low abundances throughout the YD (Fig.
561 6c), likely reflecting the variable sources of this biomarker. Finally, and again
562 consistent with observations made for 11, there is a period (ca. 11.5–9.2 cal.
563 kyr BP) following the disappearance of IP₂₅ from the record where HBI III
564 concentrations are relatively high, but this is not evident in the brassicasterol
565 profile (Fig. 6). The same combination of absent IP₂₅/high HBI III is also
566 evident between ca. 14.0–12.9 cal. kyr BP.

567

568 In summary, for each of cores 70, 11 and 1200, and for intervals where there
569 is proxy evidence for past seasonal sea ice occurrence (i.e. IP₂₅ present), the
570 relative abundances and directional changes of IP₂₅ and HBI III generally
571 oppose each other, suggesting that the observations made for these
572 biomarkers from surface sediments underlying contrasting seasonal sea ice
573 extent in the Barents Sea are replicated in downcore records. In contrast, less
574 consistent trends are observed between IP₂₅ and brassicasterol profiles,
575 probably as a result of the lower sensitivity of the latter to the overlying sea ice
576 conditions, together with likely input from other (e.g. terrestrial) sources.

577

578 4.2.4. Comparison of PIP₂₅ indices using brassicasterol and HBI III as 579 phytoplankton lipids

580

581 In addition to establishing (and interpreting) the individual biomarker profiles,
582 we also calculated PIP₂₅ indices for each of our downcore records using
583 brassicasterol and HBI III as the phytoplankton components (hereafter
584 referred to as P_BIP₂₅ and P_{III}IP₂₅, respectively). In doing so, we chose to focus
585 on the consistency (or otherwise) in outcomes using each biomarker and,
586 more specifically, the impact of the balance factor c . Thus, for each of cores
587 70, 11 and 1200, PIP₂₅ data were calculated using the method of Müller et al.
588 (2011), whereby mean sedimentary concentrations of IP₂₅ and the respective
589 phytoplankton biomarker were used to determine core-specific c values, and
590 complementary datasets, without using this term (i.e. $c=1$).

591

592 In all cases, application of the former approach yields similar outcomes when
593 using either brassicasterol or HBI III as the phytoplankton marker with, for
594 example, highest PIP_{25} values during the YD in cores 11 and 1200 (Fig. 5,6),
595 consistent with the interval of most extensive sea ice cover, and increasing
596 PIP_{25} values through the Holocene in core 70 (Fig. 4); such observations align
597 well with the conclusions based on the individual biomarker profiles. A quite
598 different picture emerges when PIP_{25} data are calculated for $c=1$, however. In
599 particular, a dramatic shift (reduction) in $P_{BIP_{25}}$ values is evident for all three
600 cores (Fig. 4-6), yet there are only very minor changes to the $P_{IIIIP_{25}}$ data. The
601 impact of such substantial (c -influenced) changes in $P_{BIP_{25}}$ values, and
602 therefore in their interpretation, is illustrated particularly well in the case of
603 core 70, where core-top $P_{BIP_{25}}$ values range from ca. 0.9 using the derived c
604 factor, to <0.1 for $c=1$ (Fig. 4), while the corresponding $P_{IIIIP_{25}}$ values are both
605 ca. 0.9, and also consistent with modern conditions (i.e. extensive sea ice
606 cover) according to the PIP_{25} categorisations of Müller et al. (2011). Of
607 course, calculation of $P_{BIP_{25}}$ using $c=1$ may be considered a somewhat
608 unrealistic scenario, especially if brassicasterol concentrations are always
609 substantially higher than those of IP_{25} . In practice, however, this is not always
610 true and, in some sediments, IP_{25} concentrations even exceed those of
611 brassicasterol (e.g. Belt et al., 2013). In any case, these examples illustrate
612 the impact that variable c can have on derived PIP_{25} data. In contrast, on the
613 basis of the data presented here, use of HBI III for PIP_{25} -based sea ice
614 estimates provides the same general outcomes to those obtained from some
615 sterol-based values, but without the complications associated with a variable c
616 factor. Determining the extent to which such an improvement on previous

617 approaches is more generally applicable, however, will require analysis of
618 downcore records from other regions and surface sediment-based
619 calibrations.

620

621 *4.2.5. Early Holocene anomalies – enhanced Atlantic Water inflow?*

622

623 For cores 11 and 1200, there are intervals during the early Holocene for which
624 IP₂₅ is absent, but where levels of HBI III are relatively high, before declining
625 and remaining low for the remainder of the records. Specifically, elevated HBI
626 III (but absent IP₂₅) occurred ca. 9.9–8.0 cal. kyr BP and ca. 11.2–9.3 cal. kyr
627 BP in cores 11 and 1200, respectively (Figs. 5, 6). This combination of IP₂₅
628 and HBI III does not occur for the northern Barents Sea site (core 70), since
629 IP₂₅ is present throughout the record (Fig. 4a). Of course, the occurrence of
630 HBI III (but not IP₂₅) is not unexpected given the ubiquity of this biomarker in
631 surface sediments from across the study region, but the elevated abundances
632 compared to modern values represents something of an anomaly and
633 requires an attempt at explanation. At this stage, since the exact sources (and
634 depth habitats) of HBI III are not known, it is not possible to conclude with
635 certainty whether its occurrence reflects near-surface or sub-surface
636 conditions, especially as the likely diatom sources inhabit a dynamic range
637 across the photic zone. Potentially, therefore, enhanced HBI III during the
638 early Holocene could be explained by increased surface layer productivity
639 during the Holocene Thermal Maximum (HTM). However, since the HTM for
640 the Nordic/Barents Seas is believed to have occurred ca. 9.0–6.0 kyr BP
641 (summarised by Risebrobakken et al., 2011), this explanation seems unlikely.

642 Alternatively, increased HBI III levels may better reflect the consequences of
643 increased Atlantic Water inflow (with associated enhanced productivity) to the
644 northern Norwegian Sea and Barents Sea, established as occurring ca.
645 10.0 ± 1.0 kyr BP (Risebrobakken et al., 2011). We note that elevated HBI III
646 concentrations (but absent IP_{25}) also occur in core 1200 during the Allerød
647 (ca. 13.8–12.9 cal. kyr BP; Fig. 6). Previously, Cabedo-Sanz et al. (2013)
648 interpreted absent IP_{25} during this interval as indicative of ice-free conditions
649 at this time, although an alternative explanation involving glacial re-advance
650 could not be discounted. Our new HBI III data are not at all consistent with
651 this latter hypothesis, however, so we conclude that ice-free conditions must
652 have prevailed during this warm interval, with environmental conditions
653 probably similar to those from ca. 11.5–9.2 cal. kyr BP.

654

655 Determination of the sources (and major environmental habitats) of HBI III is
656 clearly important, therefore, before elevated abundances of this biomarker
657 can be interpreted fully, but we suggest that quantification of this biomarker
658 has the potential to add to the existing proxies used to probe climatic and
659 oceanographic shifts in the Norwegian and Barents Seas, especially when
660 measured alongside the sea ice biomarker proxy IP_{25} .

661

662 **5. Conclusions**

663 Analysis of >100 surface sediments from diverse regions across the Barents
664 Sea has shown that the relative abundances of the diatom-derived biomarkers
665 IP_{25} and HBI III are strongly dependent on the overlying oceanographic
666 conditions, with the position of the seasonal sea ice edge playing a major role.

667 These observations are consistent with production of these biomarkers from
668 source-specific diatoms, whose habitats are strongly dependent on the
669 occurrence of seasonal sea ice. Thus, IP₂₅ appears to be produced,
670 selectively, by a small number of Arctic sea ice diatom species, while HBI III is
671 made by other diatom species, whose habitat preference appears to be
672 adjacent to the retreating sea ice edge. The potential for the combined
673 analysis of IP₂₅ and HBI III to provide more detailed assessments of past sea
674 ice conditions has been tested by their quantification in three downcore
675 records representing contrasting modern settings. The outcomes are not only
676 consistent with previous general findings, but have allowed more detailed
677 descriptions of sea conditions to be deciphered. Thus, for cores 11 and 1200,
678 high IP₂₅ and low HBI III during the YD are consistent with extensive sea
679 cover, with relatively short periods of ice-free conditions resulting from late
680 summer retreat. Towards the end of the YD (ca. 11.9 cal. kyr BP), a general
681 amelioration of conditions resulted in a near winter maximum ice edge
682 scenario, although this was somewhat variable and the eventual transition to
683 predominantly ice-free conditions was later for the western Barents Sea site
684 (core 11; ca. 9.9 cal. kyr BP) compared to NW Norway (core 1200; ca. 11.5
685 cal. kyr BP), likely as a result of its more northerly location. In contrast, the
686 northern Barents Sea site (core 70) was characterised by seasonal sea ice
687 cover throughout the Holocene with a gradual shift from winter ice edge
688 conditions during the early Holocene to more sustained ice cover in the
689 Neoglacial; a transition that has undergone something of a reverse in the last
690 ca. 150 yr according to observational records (Divine and Dick, 2006).
691

692 Our next objective will be to carry out a more detailed investigation into the
693 combined use of IP₂₅ and HBI III in some form of numerical index (e.g. PIP₂₅)
694 to ascertain whether more quantitative estimates of sea ice concentration are
695 achievable. For now, we note that surface P_{III}IP₂₅ values of 0.85 and <0.1 in
696 cores 70 and 11, respectively, are in excellent agreement with the
697 corresponding modern spring sea ice concentrations of ca. 80 and 5% (mean
698 1981-2010; NSIDC) for these two locations.

699
700 In the future, it will also be important to examine relative abundances of IP₂₅
701 and HBI III in surface and downcore records from other Arctic (and temperate)
702 regions to determine the wider applicability of this approach for detailed paleo
703 sea ice reconstruction. In this respect, we note that IP₂₅ has been reported in
704 sediments from a wide range of Arctic locations (Belt and Müller, 2013; Brown
705 et al., 2014), while HBI III is one of the most frequently occurring HBIs found
706 in marine sediments worldwide (Belt et al., 2000), likely as a result of
707 production by common diatom genera (*Pleurosigma* and *Rhizosolenia*). We
708 also note that the enhanced primary production that is characteristic of the
709 retreating sea ice edge, and identified here through the proxy biomarker HBI
710 III, is a common feature within MIZ regions across the Arctic (Perette et al.,
711 2011).

712
713 In summary, our primary aim here was to investigate the potential for selected
714 biomarkers to provide complementary (at least) information to the qualitative
715 (IP₂₅) and semi-quantitative (PIP₂₅) methods established previously. To place

716 our findings within this broader context, we propose the following assessment
717 of the current status of biomarker-based (Arctic) sea ice proxies:

718

- 719 1. The occurrence of IP₂₅ in Arctic marine sediments represents a highly
720 selective indicator of the past occurrence of seasonal sea ice cover,
721 spanning timeframes as far back as the late Pliocene (at least).
- 722 2. Substantial regional variability, in particular, means that algorithmic
723 relationships between sedimentary IP₂₅ abundance and seasonal sea
724 ice concentration are not particularly reliable; however, higher
725 IP₂₅ abundances are generally associated with enhanced sea ice extent
726 and downcore records are internally consistent (i.e. they reflect
727 directional changes in sea ice extent).
- 728 3. Semi-quantitative estimates of spring sea ice *concentration* may be
729 improved by combining IP₂₅ with other biomarkers such as those
730 biosynthesised by open-water phytoplankton; however, issues
731 regarding regional versus global calibrations still need resolving, while
732 the limitations of using a variable balance factor in calculating PIP₂₅
733 indices is particularly problematic.
- 734 4. More accurate descriptions of spring sea ice *conditions* are achievable
735 by measuring IP₂₅ alongside other source-specific biomarkers (e.g. HBI
736 III) whose production is particularly reflective of the neighbouring sea
737 ice conditions (e.g. winter sea ice margin, marginal ice zone) as shown
738 in the current study. The potential for using such a marker for more
739 semi-quantitative sea ice estimates using the PIP₂₅ (or related) index is

740 especially attractive, not least, since problems associated with using a
741 variable balance factor may be alleviated.

742

743

744 **Acknowledgments**

745 This work is a contribution to the CASE Initial Training Network funded by the
746 European Community's 7th Framework Programme FP7 2007/2013, Marie-
747 Curie Actions, under Grant Agreement No. 238111. We also thank Professor
748 Ruediger Stein (AWI) and The British Ocean Sediment Core Research Facility
749 (BOSCORF) for providing us with some of the surface sediment material (PS
750 and JR142 samples, respectively) described in this study and we are also
751 grateful to Shaun Lewin (Plymouth University) for assistance with the
752 cartography. We thank three anonymous reviewers for providing supportive
753 feedback and helpful suggestions to improve the manuscript.

754

755

756

757

758

759

760 **References**

- 761 Andrews, J.T., 2009. Seeking a Holocene drift ice proxy: non-clay mineral
762 variations from the SW to N-central Iceland shelf: trends, regime shifts,
763 and periodicities. *J. Quat. Sci.* 24, 664-676.
- 764 Aure, J., Strand, Ø., 2001. Hydrographic normals and long-term variations
765 at fixed surface layer stations along the Norwegian coast from 1936 to
766 2000, *Fisken og Havet* 13, 1-24.
- 767 Belt, S.T., Allard, W.G., Massé, G., Robert, J.-M., Rowland, S.J., 2000.
768 Highly branched isoprenoids (HBIs): Identification of the most common
769 and abundant sedimentary isomers. *Geochim.Cosmochim.Acta*64, 3839-
770 3851.
- 771 Belt, S.T., Brown, T.A., Navarro Rodriguez, A., Cabedo Sanz, P., Tonkin,
772 A., Ingle, R., 2012. A reproducible method for the extraction, identification
773 and quantification of the Arctic sea ice proxy IP₂₅ from marine
774 sediments. *Analytical Methods* 4, 705-713.
- 775 Belt, S.T., Brown, T.A., Ringrose, A.E., Cabedo-Sanz, P., Mundy, C.J.,
776 Gosselin, M., Poulin, M., 2013. Quantitative measurements of the sea ice
777 diatom biomarker IP₂₅ and sterols in Arctic sea ice and underlying
778 sediments: Further considerations for palaeo sea ice reconstruction. *Org.*
779 *Geochem.* 62, 33-45.
- 780 Belt, S.T., Massé, G., Rowland, S.J., Poulin, M., Michel, C., LeBlanc, B.,
781 2007. A novel chemical fossil of palaeo sea ice: IP₂₅. *Org. Geochem.* 38,
782 16-27.
- 783 Belt, S.T., Massé, G., Vare, L.L., Rowland, S.J., Poulin, M., Sicre, M.-A.,
784 Sampei, M., Fortier, L., 2008. Distinctive ¹³C isotopic signature
785 distinguishes a novel sea ice biomarker in Arctic sediments and sediment
786 traps. *Mar. Chem.* 112, 158-167.
- 787 Belt, S.T., Brown, T.A., Ringrose, A.E., Cabedo-Sanz, P., Mundy, C.J.,
788 Gosselin, M., Poulin, M., 2013. Quantitative measurements of the sea ice
789 diatom biomarker IP₂₅ and sterols in Arctic sea ice and underlying
790 sediments: Further considerations for palaeo sea ice reconstruction. *Org.*
791 *Geochem.* 62, 33–45.
- 792 Belt, S.T., Müller, J., 2013. The Arctic sea ice biomarker IP₂₅: a review of
793 current understanding, recommendations for future research and
794 applications in palaeo sea ice reconstructions. *Quat. Sci. Rev.* 79, 9-25.
- 795 Berben, S.M.P., 2014. A Holocene palaeoceanographic multi-proxy study
796 on the variability of Atlantic water inflow and sea ice distribution along the
797 pathway of Atlantic water. University of Tromsø (PhD thesis).
- 798 Berben, S.M.P., Husum, K., Cabedo-Sanz, P., Belt, S.T., 2014. Holocene
799 sub-centennial evolution of Atlantic water inflow and sea ice distribution in
800 the western Barents Sea, *Clim. Past*, 10, 181-198.

- 801 Brown, T.A., Belt, S.T., Tatarek, A., Mundy, C.J., 2014. Source
802 identification of the Arctic sea ice proxy IP₂₅. *Nature Communications* 5,
803 4197.
- 804 Cabedo-Sanz, P., Belt, S.T., Knies, J.K., Husum, K., 2013. Identification of
805 contrasting seasonal sea ice conditions during the Younger Dryas. *Quat.*
806 *Sci. Rev.* 79, 74-86.
- 807 Cabedo-Sanz, P., Belt, S.T., 2015. Identification and characterisation of a
808 novel mono-unsaturated highly branched isoprenoid (HBI) alkene in
809 ancient Arctic sediments. *Org. Geochem.* 81, 34-39.
- 810 Collins, L.G., Allen, C.S., Pike, J., Hodgson, D.A., Weckström, K., Massé,
811 G. 2013. Evaluating highly branched isoprenoid (HBI) biomarkers as a
812 novel Antarctic sea-ice proxy in deep ocean glacial age sediments. *Quat.*
813 *Sci. Rev.* 79, 87-98.
- 814 de Vernal, A., Gersonde, R., Goosse, H., Seidenkrantz, M.-S., Wolff, E.W.,
815 2013. Sea ice in the paleoclimate system: the challenge of reconstructing
816 sea ice from proxies – an introduction. *Quat. Sci. Rev.* 79, 1-8.
- 817 Dickson, R., Rudels, B., Dye, S., Karcher, M., Meincke, J., Yashayaev, I.,
818 2007. Current estimates of freshwater flux through Arctic and subarctic
819 seas. *Prog. Oceanogr.* 73, 210-230.
- 820 Divine, D.V., Dick, D., 2006. Historical variability of sea ice edge position in
821 the Nordic Seas. *J. Geophys. Res.* 111, C01001.
- 822 Ebbesen, H., Hald, M., 2004. Unstable Younger Dryas climate in the
823 northeast North Atlantic. *Geology* 32, 673-676.
- 824 Fahl, K., Stein, R., 2012. Modern seasonal variability and
825 deglacial/Holocene change of central Arctic Ocean sea-ice cover: New
826 insights from biomarker proxy records. *Earth Planet. Sci. Lett.* 351–352,
827 123–133.
- 828 Hald, M., Andersson, C., Ebbesen, H., Jansen, E., Klitgaard-Kristensen,
829 D., Risebrobakken, B., Salomonsen, G.R., Sarnthein, M., Sejrup, H.P.,
830 Telford, R.J., 2007. Variations in temperature and extent of Atlantic Water
831 in the northern North Atlantic during the Holocene. *Quat. Sci. Rev.* 26,
832 3423-3440.
- 833 Hopkins, T. S., 1991. The GIN Sea: A synthesis of its physical
834 oceanography and literature review, 1972-1985. *Earth Sci. Rev.* 30, 175-
835 318.
- 836 Huang, W.Y., Meinschein W.G., 1976. Sterols as source indicators of
837 organic material in sediments. *Geochim. Cosmochim. Acta* 40, 323–330.
- 838 Knies, J., 2005. Climate-induced changes in sedimentary regimes for
839 organic matter supply on the continental shelf off northern Norway.
840 *Geochim. Cosmochim. Acta* 69, 4631-4647.
- 841 Knies, J., Cabedo-Sanz, P., Belt, S.T., Baranwal, S., Fietz, S., Rosell-
842 Melé, A., 2014. The emergence of modern sea ice cover in the Arctic
843 Ocean. *Nature Communications* 5, 5608.

- 844 Knies, J., Martinez, P., 2009. Organic matter sedimentation in the western
845 Barents Sea region: Terrestrial and marine contribution based on isotopic
846 composition and organic nitrogen content. *Norwegian Journal of Geology*
847 89, 79-89.
- 848 Kvingedal, B., 2005. Sea-ice extent and variability in the Nordic Seas,
849 1967-2002, in: Drange, H., Dokken, T., Furevik, T., Gerdes, R., and
850 Berger, W. (Eds.): *The Nordic seas: An integrated perspective*, American
851 Geophysical Union, Geophysical Monograph, 158, 39-49.
- 852 Loeng, H., 1991. Features of the physical oceanographic conditions of the
853 Barents Sea, *Polar Res.*, 10, 5-18.
- 854 Maiti, K., Carroll, J., Benitez-Nelson, C.R., 2010. Sedimentation and
855 particle dynamics in the seasonal ice zone of the Barents Sea. *J. Mar.*
856 *Systems* 79, 185-198.
- 857 Massé, G., Belt, S.T., Crosta, X., Schmidt, S., Snape, I., Thomas, D.N.,
858 Rowland, S.J., 2011. Highly branched isoprenoids as proxies for variable
859 sea ice conditions in the Southern Ocean. *Antarctic Sci.* 23, 487-498.
- 860 Massé, G., Rowland, S.J., Sicre, M.-A., Jacob, J., Jansen, E., Belt, S.T.,
861 2008. Abrupt climate changes for Iceland during the last millennium:
862 Evidence from high resolution sea ice reconstructions. *Earth Planet. Sci.*
863 *Lett.* 269, 565-569.
- 864 Müller, J., Masse, G., Stein, R., Belt, S.T., 2009. Variability of sea-ice
865 conditions in the Fram Strait over the past 30,000 years. *Nature Geosci.*
866 2, 772 – 776.
- 867 Müller, J., Wagner, A., Fahl, K., Stein, R., Prange, M., Lohmann, G.,
868 2011. Towards quantitative sea ice reconstructions in the northern North
869 Atlantic: A combined biomarker and numerical modelling approach. *Earth*
870 *Planet. Sci. Lett.* 306, 137-148.
- 871 Müller, J., Werner, K., Stein, R., Fahl, K., Moros, M., Jansen, E., 2012.
872 Holocene cooling culminates in sea ice oscillations in Fram Strait. *Quat.*
873 *Sci. Rev.* 47, 1-14.
- 874 Müller, J., Stein, R., 2014. High-resolution record of late glacial sea ice
875 changes in Fram Strait corroborates ice-ocean interactions during abrupt
876 climate shifts. *Earth Planet. Sci. Lett.* 403, 446-455.
- 877 Navarro-Rodriguez, A., 2014. Reconstruction of recent and palaeo sea ice
878 conditions in the Barents Sea. University of Plymouth (PhD thesis).
- 879 Navarro-Rodriguez, A., Belt, S.T., Brown, T.A., Knies, J., 2013. Mapping
880 recent sea ice conditions in the Barents Sea using the proxy biomarker
881 IP₂₅: implications for palaeo sea ice reconstructions. *Quat. Sci. Rev.* 79, 26-
882 39.
- 883 Perette, M., Yool, A., Quartly, G.D., Popova, E.E., 2011. Near-ubiquity of ice-
884 edge blooms in the Arctic. *Biogeosciences* 8, 515-524. Doi:10.5194/bg-8-
885 515-2011.
- 886 Risebrobakken, B., T. Dokken, L.H. Smedsrud, C. Andersson, E. Jansen,
887 M. Moros, Ivanova, E.V., 2011. Early Holocene temperature variability in

- 888 the Nordic Seas: The role of oceanic heat advection versus changes in
889 orbital forcing, *Paleoceanography* 26, PA4206.
- 890 Rowland, S.J., Allard, W.G., Belt, S.T., Massé, G., Robert, J.-M.,
891 Blackburn, S., Frampton, D., Revill, A.T., Volkman, J.K., 2001. Factors
892 influencing the distributions of polyunsaturated terpenoids in the diatom,
893 *Rhizosolenia setigera*. *Phytochemistry* 58, 717-728.
- 894 Rùther, D.C., Bjarnadóttir, L.J., Junntila, J., Husum, K., Rasmussen, T.L.,
895 Lucchi, R.G., Andreassen, K., 2012. Pattern and timing of the northwestern
896 Barents Sea Ice Sheet deglaciation and indications of episodic Holocene
897 deposition. *Boreas* DOI:10.1111/j.1502-3885.2011.00244.x.
- 898 Sakshaug, E., Johnsen, G., Kristiansen, S., von Quillfeldt, C., Rey, F.,
899 Slagstad, D., Thingstad, F., 2009. Phytoplankton and primary production,
900 in: Sakshaug, E., Johnsen, G., Kovacs, K. (Eds), *Ecosystem Barents Sea*.
901 Tapir Academic Press, Trondheim, pp.167-208.
- 902 Serreze, M., Barrett, A., Slater, A., Steele, M., Zhang, J., Trenberth, K.,
903 2007. The large-scale energy budget of the Arctic. *J. Geophys. Res.*, 112,
904 D11122, doi:10.1029/2006JD008230.
- 905 Stein, R., Fahl, K., 2013. Biomarker proxy IP₂₅ shows potential for studying
906 entire Quaternary Arctic sea-ice history. *Org. Geochem.* 55, 98-102.
- 907 Stoyanova, V., Shanahan, T.M., Hughen, K.A., de Vernal, A., 2013. Insights
908 into circum-Arctic sea ice variability from molecular geochemistry. *Quat.*
909 *Sci. Rev.* 79, 63-73.
- 910 Stroeve, J.C., Serreze, M.C., Holland, M.M., Kay, J.E., Malanik, J., Barrett,
911 A.P., 2012. The Arctic's rapidly shrinking sea ice cover: a research
912 synthesis. *Clim. Change.* <http://dx.doi.org/10.1007/s10584-011-0101-1>.
- 913 Tolosa, L., Fiorini, S., Gasser, B., Martín, J., Miquel, J.C., 2013. Carbon
914 sources in suspended particles and surface sediments from the Beaufort
915 Sea revealed by molecular lipid biomarkers and compound-specific
916 isotope analysis. *Biogeosciences* 10, 2061-2087. doi:10.5194/bg-10-2061-
917 2013.
- 918 Vare, L.L., Massé, G., Gregory, T.R., Smart, C.W., Belt, S.T., 2009. Sea
919 ice variations in the central Canadian Arctic Archipelago during the
920 Holocene. *Quat. Sci. Rev.* 28, 1354-1366.
- 921 Vare, L.L., Massé, G., Belt, S.T., 2010. A biomarker-based reconstruction
922 of sea ice conditions for the Barents Sea in recent centuries. *The*
923 *Holocene*, 40, 637-643.
- 924 Vinje, T.E., 1977. Sea ice conditions in the European sector of the
925 marginal seas of the Arctic, 1966-75, *Aarb. Nor. Polarinst.* 1975, 163-174.
- 926 Volkman, J.K., 1986. A review of sterol markers for marine and terrigenous
927 organic matter. *Org. Geochem.* 9, 83-99.
- 928 Wang, Y., Cheng, H., Lawrence Edwards, R., He, Y., Kong, X., An, Z., Wu,
929 J., Kelly, M.J., Dykoski, C.A., Li, X., 2005. The Holocene Asian Monsoon:
930 Links to solar changes and North Atlantic climate. *Science* 308, 854-857.

- 931 Xiao, X., Stein, R., Fahl, K., 2013. Biomarker distributions in surface
932 sediments from the Kara and Laptev Seas (Arctic Ocean): Indicators for
933 organic-carbon sources and sea ice coverage. *Quat. Sci. Rev.* 79, 40-52.
- 934 Xiao, X., Fahl, K., Müller, J., Stein, R., 2015. Sea-ice distribution in the
935 modern Arctic Ocean: Biomarker records from trans-Arctic Ocean surface
936 sediments. *Geochim.Cosmochim.Acta*155, 16–29.
- 937
- 938

939 **Figure Legends**

940

941 Figure 1. Structures of C₂₅ highly branched isoprenoid (HBI) alkenes

942 described in the text. (I) IP₂₅; (II) C_{25:2}; (III) HBI III (C_{25:3}).

943

944 Figure 2. Map showing the study region, major surface currents and sampling

945 locations. (a) Surface currents (Red – NAC: North Atlantic Current; NCaC:

946 North Cape Current; WSC: West Spitsbergen Current; Blue – ESC: East

947 Spitsbergen Current; BIC Bear Island Current); NCC: Norwegian Coastal

948 Current; (b) Locations of surface sediments (black circles) and long cores (red

949 circles). The positions of median April and September sea ice extent (1981–

950 2010; NSIDC) are also indicated.

951

952 Figure 3. Surface sediment concentrations of (a) IP₂₅; (b) HBI III; (c)

953 brassicasterol. The positions of median April and September sea ice extent

954 (1981–2010; NSIDC), together with the maximum (1981) and minimum (2006)

955 April sea ice extent, are also indicated.

956

957 Figure 4. Downcore biomarker concentration profiles of (a) IP₂₅; (b) HBI III; (c)

958 brassicasterol in core 70 obtained from the northern Barents Sea. IP₂₅ and

959 brassicasterol data are taken from Berben (2014). PIP₂₅ profiles based on HBI

960 III (d) and brassicasterol (e) are also shown, together with the respective *c*

961 factors. The diamonds on the x-axis denote the calibrated AMS ¹⁴C

962 radiocarbon ages (Berben, 2014).

963

964 Figure 5. Downcore biomarker concentration profiles of (a) IP₂₅; (b) HBI III; (c)
965 brassicasterol in core 11 obtained from the western Barents Sea. Some of the
966 IP₂₅ and brassicasterol data are taken from Berben et al. (2014). PIP₂₅ profiles
967 based on HBI III (d) and brassicasterol (e) are also shown, together with the
968 respective *c* factors. The diamonds on the x-axis denote the calibrated AMS
969 ¹⁴C radiocarbon (Berben et al., 2014, Rütther et al., 2012). The shaded region
970 corresponds to the Younger Dryas (YD).

971

972 Figure 6. Downcore biomarker concentration profiles of (a) IP₂₅; (b) HBI III; (c)
973 brassicasterol in core 1200 obtained from the northern Norwegian Sea. IP₂₅
974 and brassicasterol data are taken from Cabedo-Sanz et al. (2013). PIP₂₅
975 profiles based on HBI III (d) and brassicasterol (e) are also shown, together
976 with the respective *c* factors. The diamonds on the x-axis denote the
977 calibrated AMS ¹⁴C radiocarbon ages. The cross indicates the Vedde Ash
978 tephra horizon used in the age model (Cabedo-Sanz et al., 2013). The shaded
979 region corresponds to the Younger Dryas (YD).

980

981

982

Disclaimer: This is a pre-publication version. Readers are recommended to consult the full published version for accuracy and citation.

Identification of paleo Arctic winter sea ice limits and the marginal ice zone:
optimised biomarker-based reconstructions of late Quaternary Arctic sea ice.

Simon T Belt ^{a,*}, Patricia Cabedo-Sanz ^a, Lukas Smik ^a, Alba Navarro-Rodriguez ^a,
Sarah M P Berben ^{b,1}, Jochen Knies ^{c,d} and Katrine Husum ^e

Highlights

- Highly branched isoprenoid (HBI) biomarkers as Arctic sea ice proxies.
- Mono-unsaturated HBI (IP₂₅) characteristic of seasonal sea ice cover.
- Tri-unsaturated HBI (HBI III) enhanced within the Marginal Ice Zone (MIZ).
- Combination of IP₂₅ and HBI III improves descriptions of sea ice conditions
- Novel proxy method applied successfully in Holocene and Younger Dryas records

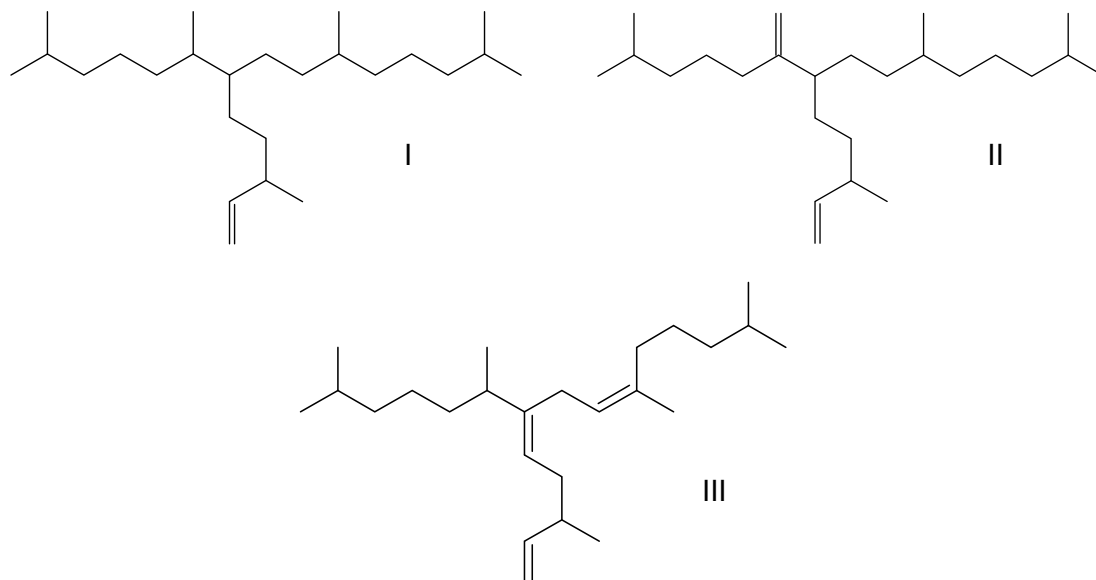
¹ Current Address: Department of Earth Science and the Bjerknes Centre for Climate Research, University of Bergen, N-5007 Bergen, Norway.

Figure

[Click here to download Figure: Figure 1.docx](#)

Disclaimer: This is a pre-publication version. Readers are recommended to consult the full published version for accuracy and citation.

Figure 1

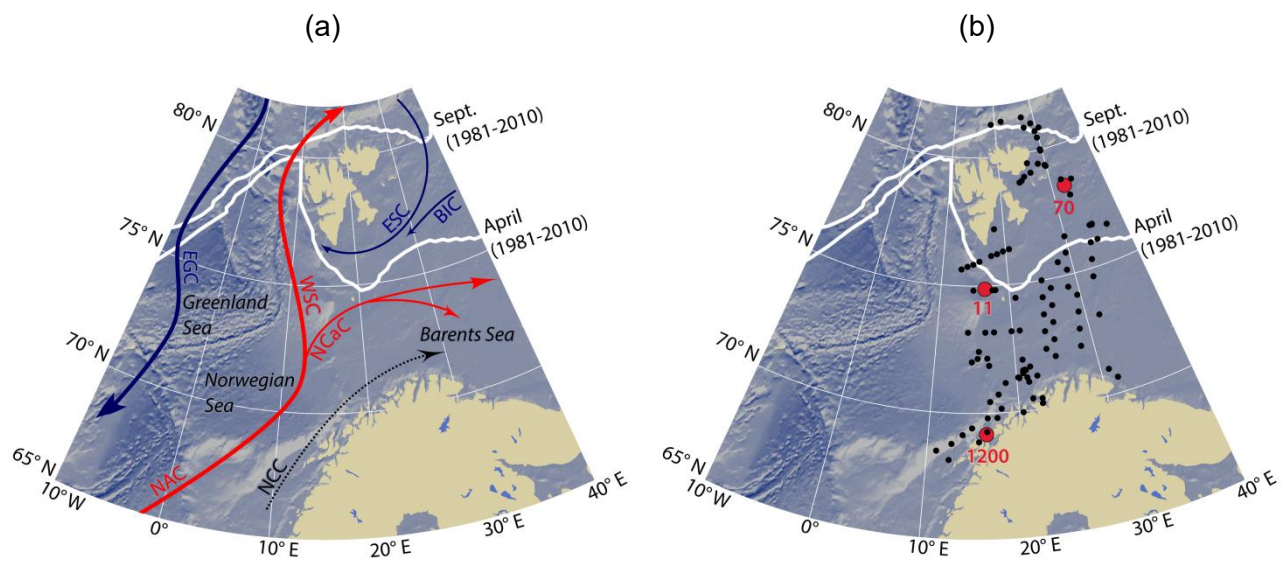


Figure

[Click here to download Figure: Figure 2.docx](#)

Disclaimer: This is a pre-publication version. Readers are recommended to consult the full published version for accuracy and citation.

Figure 2

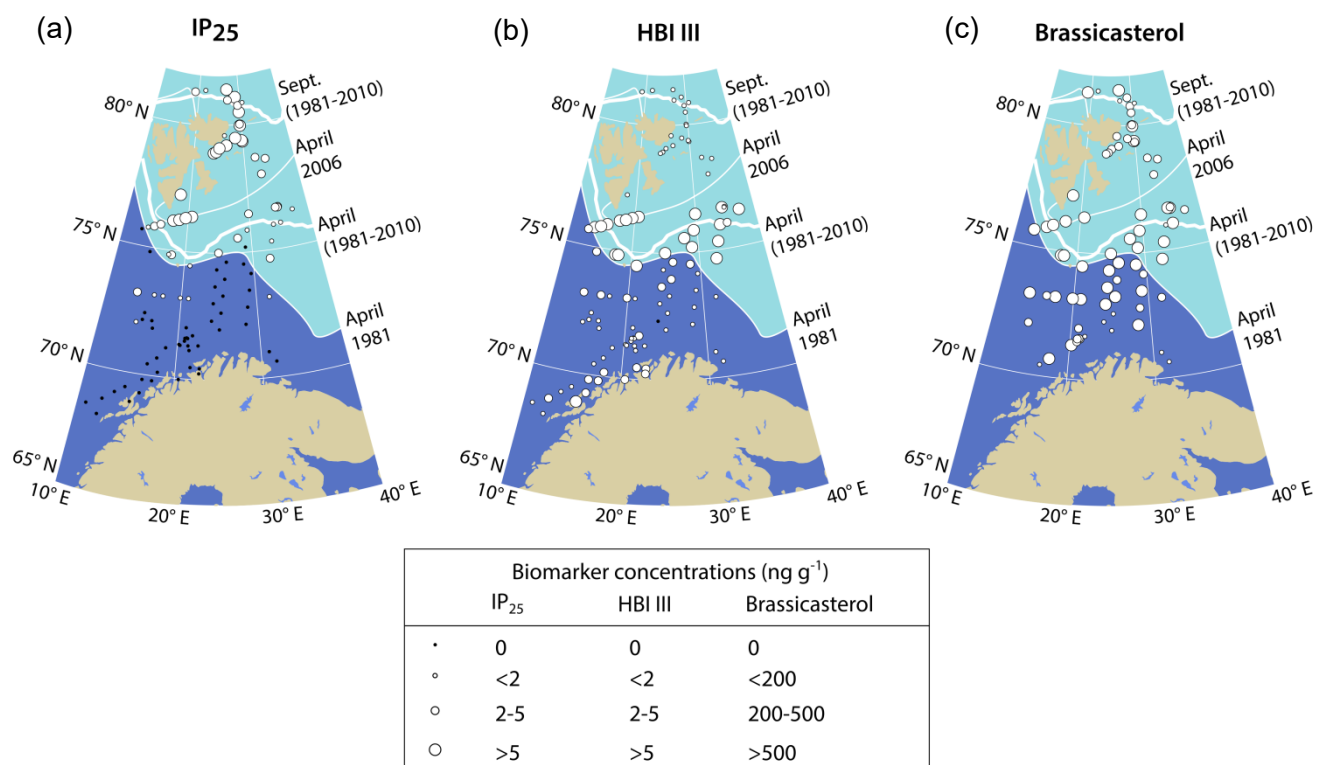


Figure

[Click here to download Figure: Figure 3.docx](#)

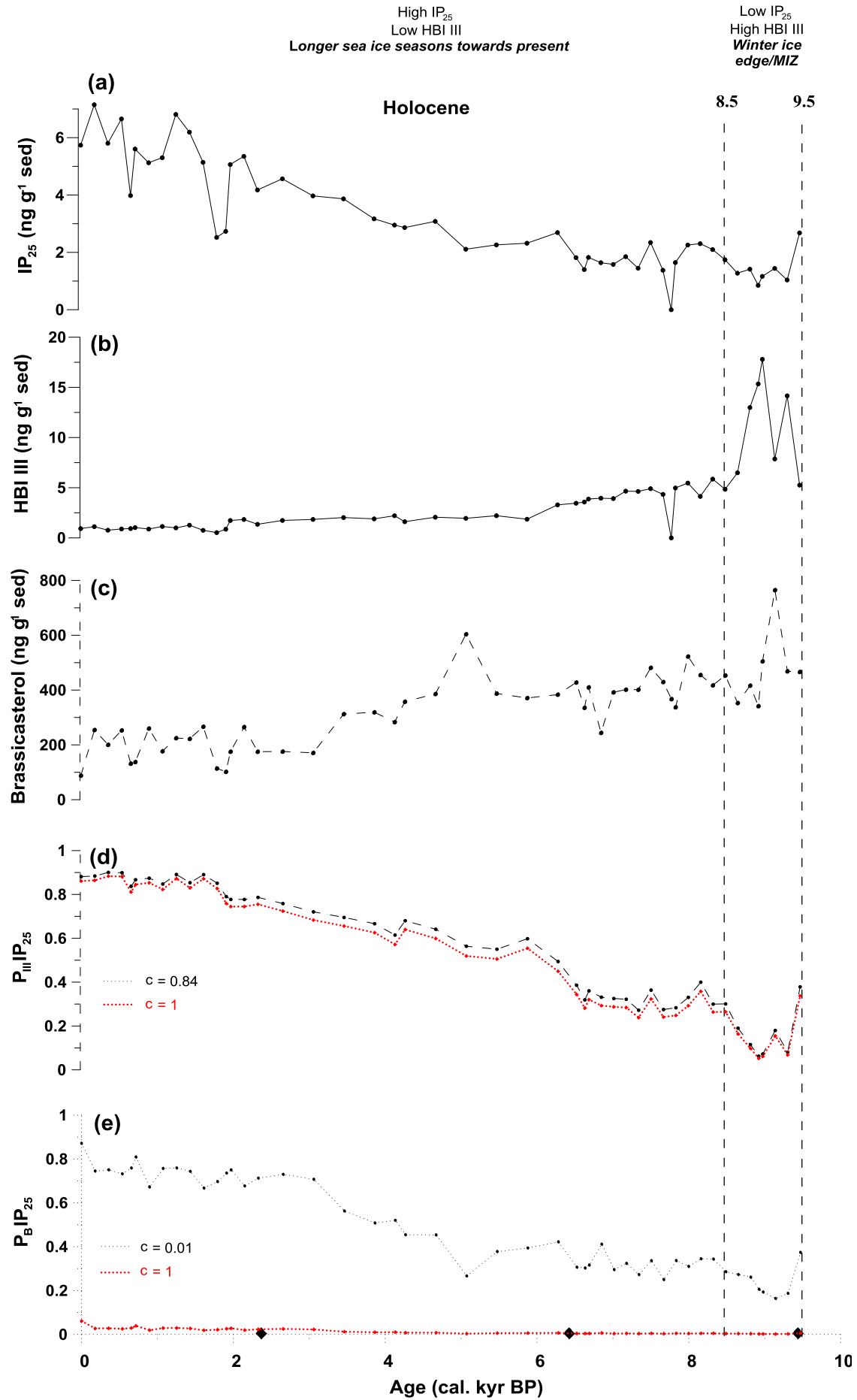
Disclaimer: This is a pre-publication version. Readers are recommended to consult the full published version for accuracy and citation.

Figure 3



Figure[Click here to download Figure: Figure 4_revised.docx](#)

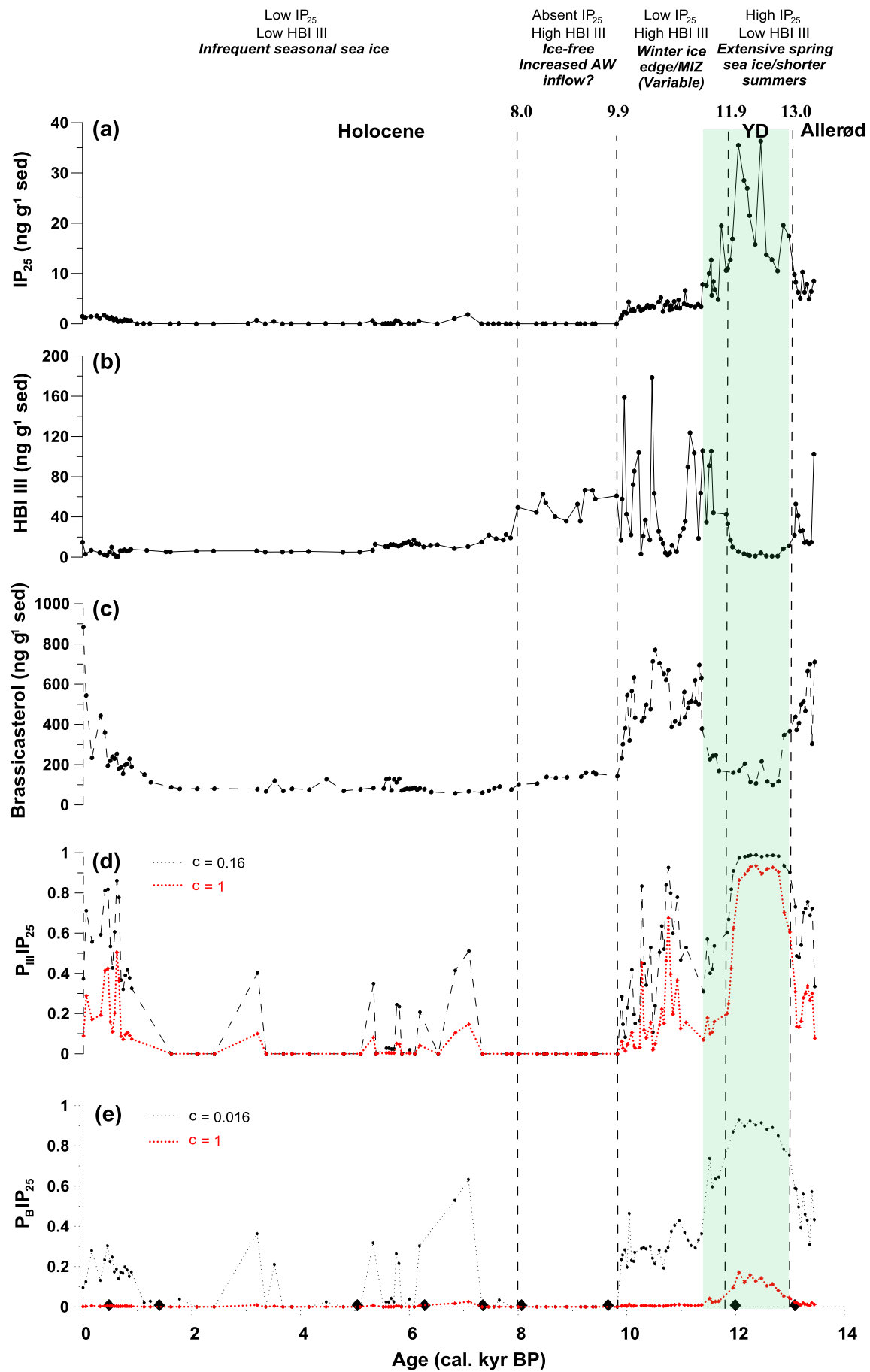
Disclaimer: This is a pre-publication version. Readers are recommended to consult the full published version for accuracy and citation.



Figure

[Click here to download Figure: Figure 5_revised.docx](#)

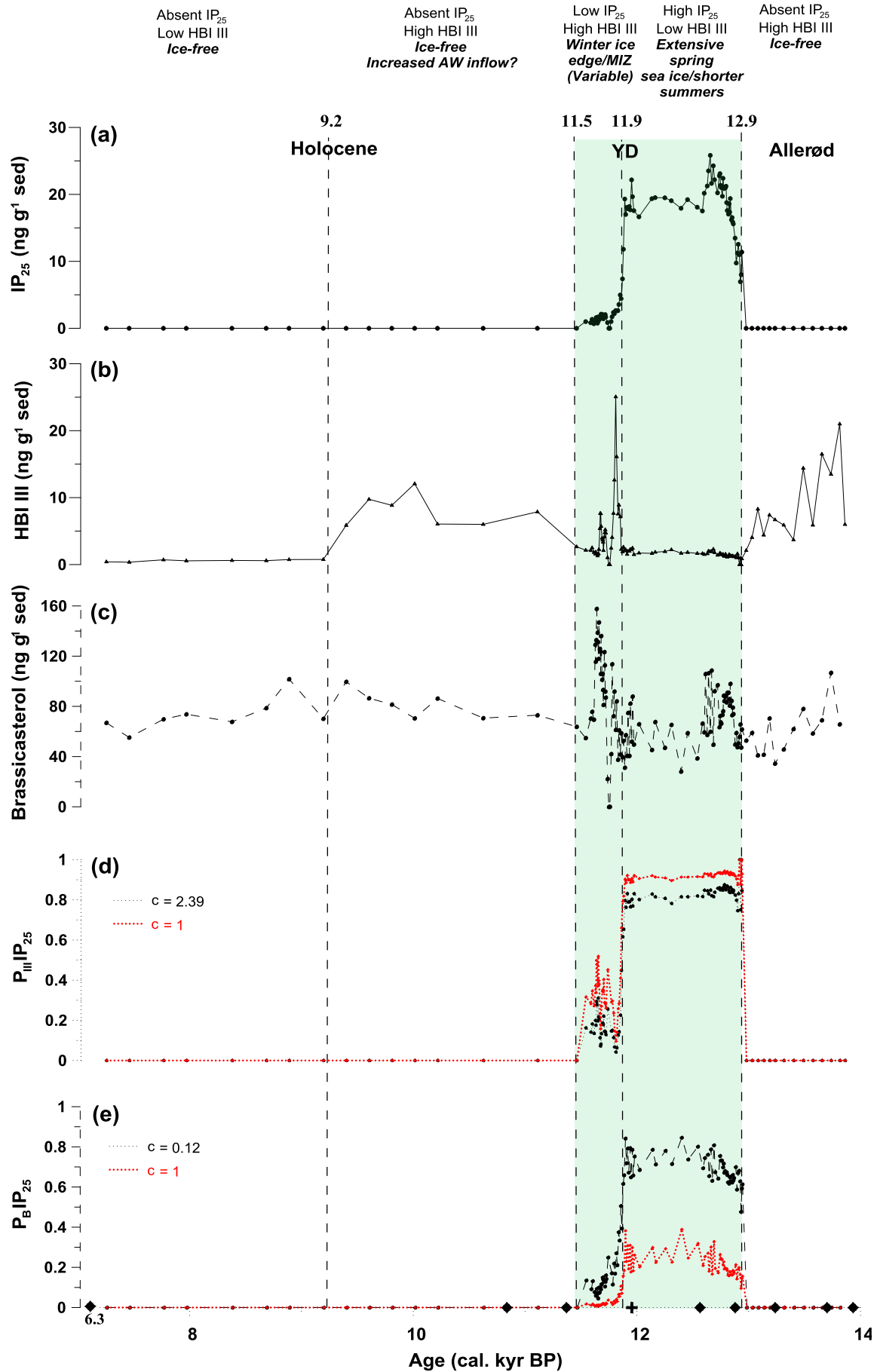
Disclaimer: This is a pre-publication version. Readers are recommended to consult the full published version for accuracy and citation.



Figure

[Click here to download Figure: Figure 6_revised.docx](#)

Disclaimer: This is a pre-publication version. Readers are recommended to consult the full published version for accuracy and citation.



Supplementary material for online publication only

[Click here to download Supplementary material for online publication only: Supplementary Table 1_revised.docx](#)

Disclaimer: This is a pre-publication version. Readers are recommended to consult the full published version for accuracy and citation.